Structure of Resonances in Electron Scattering by Hydrogen Atoms*

JOSPEH C. Y. CHEN†
University of California, San Diego, La Jolla, California
and
Joint Institute for Laboratory Astrophysics,‡ Boulder, Colorado
(Received 3 October 1966)

A study of the structure of resonances just below the $n=2$ excitation threshold in electron scattering by hydrogen atoms is carried out by utilizing an approximate method adopted from the projection-operator formalism. Analytic expressions for the level width near the threshold are obtained for both the singlet- and triplet-compound-state series with zero total angular momentum. It is found that the level widths behave like the level spacings in that they decrease exponentially as the levels approach the threshold. Nevertheless, the ratio between the level spacings and widths remains a constant less than 1. It is then concluded from the study that within the approximations adopted in the method, neither the singlet nor triplet series of the compound states become overlapping near the threshold. However, the Lamb shift may, by removing the degeneracy in the $n=2$ levels, cut off these infinite sequences of compound states, thereby restricting the number of allowed resonances. The interference between potential and resonance scatterings is also examined.

I. INTRODUCTION

In recent years, a number of resonances in the elastic electron scattering by atoms and molecules have been found theoretically and observed experimentally.[1–6] In the present paper we deal with the simplest case of such scattering systems, namely, electron scattering by hydrogen atoms. The existence of resonance in the elastic electron-hydrogen scattering system (H,e) just below the $n=2$ excitation threshold was first predicted by Burke and Schey[2] in a detailed close-coupling calculation. Subsequently, a number of theoretical papers, in which various methods are discussed,[3–5] have appeared; these papers confirm this prediction. Experimental observation of such a compound state was later reported by Schulz, by Kleinpopen and Raible, and by McGowan, Clarke, and Curley.[6]

The structure of the resonance is, however, not well understood. It was first pointed out by Gailitis and Damburg[4] that because of the strong electric dipole interaction between the projectile electron and the degenerate $n=2$ levels of hydrogen, there may exist an infinite number of resonances in the (H,e) scattering system just below the $n=2$ excitation threshold. However, the Lamb shift may, by removing the degeneracy in the $n=2$ levels, cut off this infinite sequence of compound states, thereby restricting the number of allowed resonances. The pertinent question is then whether these allowed resonances are isolated or overlapping. The purpose of this paper is to present a study concerning this question.

The plan of the paper is as follows. In Sec. II, a very brief review of Feshbach's treatment of resonances[7] which leads naturally to the expression for the resonance width is given for a two-electron system. By utilizing the derived expressions, a study of resonance structure is carried out in subsequent sections. In Sec. III, the method used to obtain the channel wave function is outlined. The determination of the compound channel wave function is described in Sec. IV in which an effective one-particle Schrödinger equation is derived for the projectile electron in a zero total angular momentum scattering. The potential in the effective Schrödinger equation is constructed in such a way that it asymptotically takes the appropriate electric dipole form arising from the interaction with the degenerate $n=2$ target levels and in such a way that it is capable of reproducing the calculated level positions of the lowest $L=0$ singlet and triplet compound states. In Sec. V, level positions of higher members of the two series are

* Work supported in part by the Advanced Research Projects Agency (Project DEFENDER) and was monitored by the U. S. Army Research Office–Durham under Contract DA-31-124-ARO-D-257.

† Joint Institute for Laboratory Astrophysics Visiting Fellow (1965-1966). Present address: Department of Physics and Insititute for Radiation Physics and Aerodynamics, University of California at San Diego, La Jolla, California.

‡ Of the National Bureau of Standards and University of Colorado.

[1] (a) For atomic systems, see for example, S. Silverman and E. N. Lassetre, Ohio State University Research Foundation Report No. 9, 1958 (unpublished); G. J. Schulz, Phys. Rev. Letters **10**, 104 (1963); R. P. Madden and K. Codling, *ibid.* **10**, 516 (1963); J. A. Simpson and U. Fano, *ibid.* **11**, 158 (1963); C. E. Kuyatt, S. R. Mielczarek, and J. A. Simpson, *ibid.* **12**, 293 (1964); J. A. Simpson, S. R. Mielczarek, and J. W. Cooper, J. Opt. Soc. Am. **54**, 269 (1964); E. Holøien and J. Midtdal, J. Chem. Phys. **45**, 2209 (1966). (b) For molecular systems, see for example, G. J. Schultz, Phys. Rev. **135**, A988 (1964); J. C. Y. Chen, *ibid.* **146**, 61 (1966); C. E. Kuyatt, J. A. Simpson, and S. R. Mielczarek, J. Chem. Phys. **44**, 437 (1966).

[2] P. G. Burke and H. M. Schey, Phys. Rev. **126**, 149 (1962).

[3] K. Smith, R. P. McEachran, and P. A. Frazer, Phys. Rev. **125**, 553 (1962); M. H. Mittleman, Phys. Rev. Letters **10**, 145 (1962); R. P. McEachran and P. A. Frazer, Proc. Phys. Soc. (London) **82**, 1038 (1963); A. Temkin and R. Pohle, Phys. Rev. Letters **10**, 22 (1963); A. Herzenberg and F. Mandl, Proc. Roy. Soc. (London) **274**, 253 (1963).

[4] M. Gailitis and R. Damburg, Proc. Phys. Soc. (London) **82**, 192 (1963).

[5] T. F. O'Malley and S. Geltman, Phys. Rev. **137**, A1344 (1965).

[6] (a) G. J. Schulz, Phys. Rev. Letters **13**, 583 (1964); (b) H. Kleinpopen and V. Raible, Phys. Letters **18**, 24 (1965); (c) J. W. McGowan, E. M. Clarke, and E. K. Curley, Phys. Rev. Letters **15**, 917 (1965); **17**, 66 (1966).

[7] H. Feshbach, Ann. Phys. (N. Y.) **5**, 387 (1958); **19**, 287 (1962).

calculated from the dispersion relation of the effective one-particle equation and are compared with other available theoretical values. The ratio formula of the level positions near the threshold derived by Gailitis and Damburg[4] is then normalized so that an analytical expression of the level spacings is derived (in Sec. VI). Level widths are calculated in Sec. VI where a comparison is made with a measured width[8] and with values calculated using other approximations. An analytic expression for the level widths near the threshold is derived, and it is found that widths behave like spacings in that they decrease exponentially as the levels approach the threshold. By utilizing these derived expressions for level spacings and widths, the structure of the resonances is then examined. The profile of the cross section is calculated in Sec. VII. Finally, in Sec. VIII, some concluding remarks are stated.

II. EXPRESSION FOR THE WIDTH OF COMPOUND STATES

The Schrödinger equation which represents a two-electron scattering system is

$$(H-E)\Psi=0, \tag{2.1}$$

where the Hamiltonian, neglecting the relativistic and finite-mass effects, may be written in terms of the center-of-mass coordinates as

$$H=H_0(\mathbf{r}_1)+H_0(\mathbf{r}_2)+V_0(\mathbf{r}_1,\mathbf{r}_2). \tag{2.2}$$

The total wave function Ψ for the two-electron system is antisymmetrical with respect to interchanging electron coordinates, including spin coordinates. Since we are dealing with a nonrelativistic two-electron system with no external magnetic interaction, we may suppress the explicit dependence of the wave function on spin coordinates and carry the total spin S as a parameter so that

$$\Psi(\mathbf{r}_1,\mathbf{r}_2)=(-)^S\Psi(\mathbf{r}_2,\mathbf{r}_1). \tag{2.3}$$

Let $\chi_\nu(\mathbf{r})$ denote the target states in configuration space having the corresponding eigenvalues ϵ_ν; then

$$H_0(\mathbf{r})\chi_\nu(\mathbf{r})=\epsilon_\nu\chi_\nu(\mathbf{r}), \tag{2.4}$$

where ν denotes the set of hydrogenic quantum numbers (n,l,m) and

$$\chi_\nu(\mathbf{r})=r^{-1}\chi_{nl}(r)Y_l{}^m(\hat{r}). \tag{2.5}$$

We let $\nu=1$ denote the ground state and set $\epsilon_1=\frac{1}{2}$ to define our energy scale.[9]

For elastic scattering, we may project out, from the total wave function Ψ, the elastic channel involving only the ground target state and treat the remainder of Ψ as a field for generating nonlocal optical potentials for the elastic channel. To do this, we require a projection operator P such that

$$P\Psi=\chi_1(\mathbf{r}_1)\mathfrak{U}_1(\mathbf{r}_2)+(-)^S\chi_1(\mathbf{r}_2)\mathfrak{U}_1(\mathbf{r}_1) \tag{2.6}$$

with the remainder of Ψ [i.e., $Q\Psi$, $Q=1-P$] given by

$$Q\Psi=\sum_{\nu\neq1}\{\chi_\nu(\mathbf{r}_1)\mathfrak{U}_\nu(\mathbf{r}_2)+(-)^S\chi_\nu(\mathbf{r}_2)\mathfrak{U}_\nu(\mathbf{r}_1)\}, \tag{2.7}$$

where the completeness relation $\sum_\nu|\chi_\nu(\mathbf{r})\rangle\langle\chi_\nu(\mathbf{r})|=1$ is implied. The appropriate projection operator P which is Hermitian and idempotent is[10]

$$P=P_1(\mathbf{r}_1)+P_1(\mathbf{r}_2)-P_1(\mathbf{r}_1)P_1(\mathbf{r}_2), \tag{2.8}$$

where $P_\nu=|\chi_\nu(\mathbf{r})\rangle\langle\chi_\nu(\mathbf{r})|$ is the elementary projection operator. This permits us to define the single-particle channel wave function $\mathfrak{U}_\nu(\mathbf{r}_j)$ uniquely in terms of the inner product $\langle\chi_\nu(\mathbf{r}_i)|\Psi(\mathbf{r}_i,\mathbf{r}_j)\rangle$ (Appendix A):

$$\mathfrak{U}_\nu(\mathbf{r}_j)=\tfrac{1}{2}[1+\delta_{\nu1}-P_1(\mathbf{r}_j)]\langle\chi_\nu(\mathbf{r}_i)|\Psi(\mathbf{r}_i,\mathbf{r}_j)\rangle, \tag{2.9}$$

where $\delta_{\mu1}=\delta_{n1}\delta_{l0}\delta_{m0}$ are the delta functions. It may easily be shown that the single-particle channel wave functions $\mathfrak{U}_\nu$ defined by Eq. (2.9) are orthogonal to the ground target state χ_1 for $\nu\neq1$ and satisfy the boundary conditions inferred by Ψ:

$$\mathfrak{U}_\nu(\mathbf{r})\underset{r\to\infty}{\longrightarrow}\delta_{\nu1}e^{ik_1z}+f_\nu(\hat{k}_i,\hat{r})\frac{e^{ik_ir}}{r}, \tag{2.10}$$

where the k's are the wave number of the electron and the f_ν's are the scattered amplitudes.

Since P projects out the complete elastic channel from Ψ, it then follows that $Q\Psi$ does not contain any incident wave. Thus, the Schrödinger equation (2.1) may be solved for $P\Psi$ in terms of Q yielding[7]

$$(\mathcal{H}-E)P\Psi=0, \tag{2.11}$$

with

$$\mathcal{H}=P\left\{H+HQ\frac{1}{E-QHQ}QH\right\}P. \tag{2.12}$$

The explicit appearance of the resonance energies in the effective Hamiltonian $\mathcal{H}$ comes from the bound states of the Q-projected Hamiltonain QHQ

$$(QHQ-\mathcal{E}_\alpha)Q\Phi_\alpha=0, \tag{2.13}$$

where the $Q\Phi_\alpha$'s approximate the quasistationary nature of the compound states. Thus, the eigenvalues so obtained approximate the level positions of the compound states.

For an isolated resonance, Eq. (2.11) may be written as

$$(E-\mathcal{H}')P\Psi=PHQ\frac{|\phi_\alpha\rangle\langle\phi_\alpha|}{E-\mathcal{E}_\alpha}QHP\Psi, \tag{2.14}$$

with

$$\mathcal{H}'=\mathcal{H}-PHQ\frac{|\phi_\alpha\rangle\langle\phi_\alpha|}{E-\mathcal{E}_\alpha}QHP. \tag{2.15}$$

[8] J. W. McGowan, following paper, Phys. Rev. **156**, 165 (1967).
[9] Atomic units are used throughout this paper except where indicated otherwise.
[10] Y. Hahn, T. F. O'Malley, and L. Spruch, Phys. Rev. **128**, 932 (1962).

Solving Eq. (2.14) for $P\Psi$, we obtain

$$P\Psi = P\psi^{(+)} + \frac{1}{E-\mathcal{H}'+i\eta}\Lambda PHQ\Phi_\alpha \tag{2.16}$$

with

$$\Lambda = \frac{\langle\Phi_\alpha|QHP|\psi^{(+)}\rangle}{E-\mathcal{E}_\alpha-\langle\Phi_\alpha QHP[1/(E-\mathcal{H}'+i\eta)]PHQ\Phi_\alpha\rangle}, \tag{2.17}$$

where $P\psi^{(\pm)}$ is the homogeneous solution of Eq. (2.14):

$$(\mathcal{H}'-E)P\psi^{(\pm)}=0. \tag{2.18}$$

The structure of the resonance is given by Λ [Eq. (2.17)] which may be interpreted as the probability of compound-state formation. From the definition of the complex resonance energy, we find from the denominator of Eq. (2.17):

$$\mathcal{W}_\alpha \equiv \mathcal{E}_\alpha' - \tfrac{1}{2}i\Gamma_\alpha$$
$$= \mathcal{E}_\alpha + \left\langle \Phi_\alpha QHP \frac{1}{E-\mathcal{H}'+i\eta} PHQ\Phi_\alpha \right\rangle. \tag{2.19}$$

This permits us to write for the resonance energy $\mathcal{E}'_\alpha$

$$\mathcal{E}_\alpha' = \mathcal{E}_\alpha + \left\langle \Phi_\alpha QHP\mathcal{P}\frac{1}{E-\mathcal{H}'} PHQ\Phi_\alpha \right\rangle \tag{2.20}$$

and for the width

$$\Gamma_\alpha = 2\pi\langle\Phi_\alpha QHP\delta(E-\mathcal{H}')PHQ\Phi_\alpha\rangle. \tag{2.21}$$

Utilizing the outgoing solutions of Eq. (2.18), the width given by Eq. (2.21) takes the expression

$$\Gamma_\alpha = 2\pi\int |\langle\psi^{(-)}|PHQ|\Phi_\alpha\rangle|^2\rho d\Omega_f \tag{2.22}$$

with

$$\rho = \frac{1}{(2\pi)^3}\left(\frac{k_f^2 dk_f}{dE_{k_f}}\right), \quad f=(i,1), \tag{2.23}$$

where k_f is the wave number of the electron in the exit channel, and the operator $\int d\Omega_f\rho$ accounts for decaying of the electron into all the infinitesimal elements of the solid angle $d\Omega_f$ in the exit channel. For elastic scattering, the only open channel is $(k_{i\nu},\nu)$ with $\nu=1$ which is spherically symmetrical; the expression for the width reduces to

$$\Gamma_\alpha = (k_f/\pi)|\langle\psi^{(-)}|PHQ|\Phi_\alpha\rangle|^2$$
$$= (k_f/\pi)|\langle P\psi^{(-)}|V_0|Q\Phi_\alpha\rangle|^2, \tag{2.24}$$

where we used Eq. (2.2) and the relations $PQ=0$ and $[P,H_0]=[Q,H_0]=0$.

For overlapping resonances, the situation becomes, however, more complicated. The formal solution of Eq. (2.11) now takes the form

$$P\Psi = P\psi^{(+)} + \frac{1}{E-\mathcal{H}''+i\eta}\sum_\alpha \Lambda_\alpha PHQ\Phi_\alpha \tag{2.25}$$

with

$$\mathcal{H}'' = \mathcal{H} - PHQ\sum_\alpha \frac{|\Phi_\alpha\rangle\langle\Phi_\alpha|}{E-\mathcal{E}'_\alpha}QHP, \tag{2.26}$$

where the resonance structure functions Λ_α have no longer the simple expression given by Eq. (2.17) but must be determined by solving the set of simultaneous equations

$$\sum_{\alpha'}\left\{(E-\mathcal{E}_\alpha')\delta_{\alpha\alpha'} - \left\langle \Phi_\alpha QHP\frac{1}{E-\mathcal{H}''+i\eta}PHQ\Phi_{\alpha'}\right\rangle\right\}\Lambda_{\alpha'}$$
$$= \langle\phi_\alpha|QHP|\psi^{(+)}\rangle. \tag{2.27}$$

It is clear that Eq. (2.27) reduces to Eq. (2.17) for isolated resonance. For overlapping resonances, it is convenient to introduce the concept of averaged width $\langle\Gamma\rangle$ such that

$$\langle\Gamma\rangle = (2\pi/N)\sum_{\alpha'}\langle\Phi_{\alpha'}QHP\delta(E-\mathcal{H}'')PHQ\Phi_{\alpha'}\rangle, \tag{2.28}$$

where N is the number of overlapping compound states.

III. DETERMINATION OF $P\psi$

In order to carry out the calculation for the width from Eq. (2.24), both the channel wave function $P\psi$ and the quasi-stationary representation $Q\Phi_\alpha$ of the compound-state wave function must be determined. In this section, we deal with the determination of the channel wave function $P\psi$. The determination of $Q\Phi_\alpha$ will be given in the next section. We now concentrate our discussion throughout the rest of the paper on the (e,H) system.

Since the projection operator P given by Eq. (2.8) commutes with the target Hamiltonian H_0, the Schrödinger equation (2.18) may be rewritten as

$$\{E-H_0(\mathbf{r}_1)-H_0(\mathbf{r}_2)\}P\psi = PVP\psi, \tag{3.1}$$

with

$$V = V_0 + HQ\left\{\frac{1}{E-QHQ} - \frac{|\Phi_\alpha\rangle\langle\Phi_\alpha|}{E-\mathcal{E}_\alpha'}\right\}QH, \tag{3.2}$$

where in the potential V the first term V_0 is simply the interelectronic repulsive potential $|\mathbf{r}_1-\mathbf{r}_2|^{-1}$ and the remaining term in V is the nonlocal optical potential including the effects of distant resonances. From the definition of the projection operator P [Eqs. (2.6) and (2.8)], $P\psi$ may be written as

$$P\psi = (2\pi)^{1/2}\{\chi_1(\mathbf{r}_1)v_1(\mathbf{r}_2)+(-)^S\chi_1(\mathbf{r}_2)v_1(\mathbf{r}_1)\}, \tag{3.3}$$

with

$$v_1(\mathbf{r}_j) = [1-\tfrac{1}{2}P_1(\mathbf{r}_j)]\langle\chi_1(\mathbf{r}_i)|\psi(\mathbf{r}_i,\mathbf{r}_j)\rangle, \tag{3.4}$$

where v_1 is the single-particle channel wave function corresponding to the Hamiltonain $\mathcal{H}'$, and $(2\pi)^{1/2}$ comes from the normalization of v_1 and $P\psi$.

To remove the angular parts of Eq. (3.1), we expand the channel wave function $v_1(r)$ in spherical harmonics

$$v_1(\mathbf{r})=\sum_{l_2m_2}\langle 0l_20m_2|LM\rangle r^{-1}v_{k_1l_2}(r)Y_{l_2}{}^{m_2}(\hat{r}), \quad (3.5)$$

where L and M are the total orbital and magnetic angular momenta of the scattering system, respectively, and the $\langle l_il_jm_im_j|LM\rangle$'s are the Clebsch-Gordan coefficients. Substituting $P\psi$ from Eq. (3.3) into Eq. (3.1) with v_1 given by Eq. (3.5) and operating on the resultant equation by $\sum_{m_2}\langle 0l_2'0m_2'|LM\rangle \times\langle Y_{l_1'}{}^{m_2'}(\hat{r}_2)|$, we obtain

$$\left\{\frac{d^2}{dr_2{}^2}-\frac{l_2(l_2+1)}{r_2{}^2}+2V_1(r_2)+k_1{}^2\right\}v_{k_1l_2}(r_2) =2K_1(r_2,r_1)v_{k_1l_2}(r_1), \quad (3.6)$$

where

$$k_1{}^2=2(E-\epsilon_1)=k_1{}^2+1, \quad (3.7)$$

$$V_1(r_2)=\frac{1}{r_2}\sum_{l_2'm_2'm_2}\langle 0l_20m_2|LM\rangle \times\langle 0l_2'0m_2'|LM\rangle\langle Y_{l_2}{}^{m_2}(\hat{r}_2)|\langle\chi_1(\mathbf{r}_1)| \times V(\mathbf{r}_1,\mathbf{r}_2)|\chi_1(\mathbf{r}_1)\rangle|Y_{l_2'}{}^{m_2'}(\hat{r}_2)\rangle, \quad (3.8)$$

$$K_1(r_2,r_1)v_{k_1l_2}(r_1)=(-)^{S-L}\chi_{10}(r_2)\sum_{l_2'm_2'm_2}(-)^{l_2'} \times\langle 0l_20m_2|LM\rangle\langle 0l_2'0m_2'|LM\rangle\langle Y_{l_2}{}^{m_2}(\hat{r}_2)| \times\langle\chi_1(\mathbf{r}_1)|V(\mathbf{r}_1,\mathbf{r}_2)-\tfrac{1}{2}(1+k_1{}^2) \times|v_{k_1l_2}(r_1)Y_{l_2'}{}^{m'}(\hat{r}_1)\rangle|Y_0{}^0(\hat{r}_2)\rangle. \quad (3.9)$$

Equation (3.6) differs from the static-exchange equation[11] in the appearance of the nonlocal optical potential. However, if we approximate V [Eq. (3.2)] by its first term V_0 (i.e., equivalent to the static approximation $H'\cong PHP$), Eq. (3.6) reduces to the static-exchange approximation.[11]

$$\left[\frac{d^2}{dr_2{}^2}-\frac{l_2(l_2+1)}{r_2{}^2}+2\left(1+\frac{1}{r_2}\right)e^{-2r_2}+k_1{}^2\right]v_{k_1l_2}(r_2) =\mathcal{W}_{k_1L}{}^{(S)}(r_2), \quad (3.10)$$

where

$$\mathcal{W}_{k_1L}{}^{(S)}(r_2)=\frac{2(-)^S}{2L+1}\chi_{10}(r_2)\left\{\int_0^{r_2}\chi_{10}(r_1)\left(\frac{r_1{}^L}{r_2{}^{L+1}}-\frac{r_2{}^L}{r_1{}^{L+1}}\right) \times v_{k_1l_2}(r_1)dr_1+r_2{}^L\int_0^{\infty}\chi_{10}(r_1) \times\left[\frac{1}{r_1{}^{L+1}}+\tfrac{1}{2}(1+k_1{}^2)\delta_{L0}\right]v_{k_1l_2}(r_1)dr_1\right\}. \quad (3.11)$$

[11] P. M. Morse and W. P. Allis, Phys. Rev. 44, 269 (1933); B. H. Bransden, A. Dalgarno, T. L. John, and M. J. Seaton, Proc. Phys. Soc. (London) 71, 877 (1958).

The integro-differential equation (3.10) is solved numerically for $v_{k_1k_2}(r_2)$ subject to the boundary conditions

$$v_{k_1l_2}(r_2=0)=0, \quad (3.12)$$

$$v_{k_1l_2}(r_2)\underset{r\to\infty}{\longrightarrow}k_1{}^{-1}\sin(k_1r-L\tfrac{1}{2}\pi+\tilde{\delta}_L{}^{(S)}), \quad (3.13)$$

where the $\tilde{\delta}_L{}^{(S)}$'s are the phase shifts. It is well known that the phase shift so obtained does not give the correct potential scattering, since the neglected nonlocal potential is of importance in potential scattering. However, for the purpose of calculating width, the static-exchange wave function obtained from Eq. (3.10) may constitute a reasonable approximation, since at resonance the dominating distortion which arises from compound-state formation is accounted for in the Q subspace. The accuracy of the calculated width from this approximate wave function is discussed in Sec. VI where comparisons with other approximations are made.

IV. DETERMINATION OF $Q\Phi_\alpha$

The stationary representation of the compound state may be obtained from the Q-projected Schrödinger equation

$$(QHQ-\mathcal{E}_\alpha)Q\Phi_\alpha=0, \quad (4.1)$$

where $Q\Phi_\alpha$ has no ground target-state component:

$$Q\Phi_\alpha=\sum_{\nu\neq 1}\{\chi_\nu(\mathbf{r}_1)\phi_{\nu\alpha}(\mathbf{r}_2)+(-)^S\chi_\nu(\mathbf{r}_2)\phi_{\nu\alpha}(\mathbf{r}_1)\}. \quad (4.2)$$

From the definition of the projection operator Q, the single-particle compound wave functions $\phi_{\nu\alpha}(r_j)$ take the form

$$\phi_{\nu\alpha}(\mathbf{r}_j)=\tfrac{1}{2}[1-P_1(\mathbf{r}_j)]\langle\chi_\nu(\mathbf{r}_i)|\Phi_\alpha(\mathbf{r}_i,\mathbf{r}_j)\rangle. \quad (4.3)$$

In actual applications, only a finite number of excited target states may be included in Eq. (4.2); it is then no longer possible to satisfy Eq. (4.1). For such cases, we may vary $Q\Phi_\alpha$ (*i.e.*, vary $\phi_{\nu\alpha}$ in the subspace projected by Q) so that

$$\delta\langle Q\Phi_\alpha|QHQ-\mathcal{E}_\alpha|Q\Phi_\alpha\rangle=0. \quad (4.4)$$

This is equivalent to making the single-particle compound wave function $\phi_{\nu\alpha}$ satisfy the Hartree-Fock equations. Equation (4.4) may also be solved by constructing the appropriate parametrized trial variational wave function for $Q\Phi_\alpha$ and minimizing the variational parameters[5] or by solving a first-order matrix differential equation representing the resultant coupled equations.[12]

Expanding $\phi_{\nu\alpha}$ in spherical harmonics, one obtains [remembering $\nu=(n,l,m)$]

$$\phi_{\nu\alpha}(\mathbf{r}_j)=\sum_{l_j,m_j}\langle l_il_jm_im_j|LM\rangle r_j{}^{-1}\phi_{k_n\alpha l_j}(r_j)Y_{l_j}{}^{m_j}(\hat{r}_j). \quad (4.5)$$

Now if we substitute $Q\Phi_\alpha$ from Eq. (4.2) with the

[12] J. C. Y. Chen, J. Math. Phys. 6, 1723 (1965).

$\phi_{\nu\alpha}$'s given by Eq. (4.5) into Eq. (4.4), and if we carry out the variation inside the integral and then integrate the resultant over the approximate coordinates, we obtain

$$\left\{\frac{d^2}{dr_2^2}-\frac{l_2(l_2+1)}{r_2^2}+k_{n\alpha}^2\right\}\phi_{kn\alpha l_2}=2\sum_{n\ l_1'l_2'}\{V_{nl_1l_2}^{\ n'l_1'l_2'}(r_2)\phi_{kn'\alpha l_2'}(r_2)+K_{nl_1l_2}^{\ n'l_1'l_2'}(r_2,r_1)\phi_{kn'\alpha l_2'}(r_1)\} \tag{4.6}$$

with

$$k_{n\alpha}^2=2(\mathcal{E}_\alpha-\epsilon_n)\,,\qquad n>1\,, \tag{4.7}$$

$$V_{nl_1l_2}^{\ n'l_1'l_2'}(r_2)=-\delta_{\nu\nu'}\frac{1}{r_2}+\sum_\beta f_\beta(l_1l_2,l_1'l_2';L)\int\chi_{nl_1}(r_1)\frac{r^{<\beta}}{r_>^{\beta+1}}\chi_{n'l_1'}(r_1)dr_1\,, \tag{4.8a}$$

$$K_{nl_1l_2}^{\ n'l_1'l_2'}(r_2,r_1)\phi_{kn'\alpha l_2'}(r_1)=(-)^S\chi_{n'l_1'}(r_2)\sum_\beta g_\beta(l_1l_2,l_1'l_2';L)$$
$$\times\int\chi_{nl_1}(r_1)\left[\frac{r_<^\beta}{r_>^{\beta+1}}-\left(\frac{1}{2n'}+\frac{k_{n\alpha}^2}{2}\right)\delta_{\beta0}\right]\phi_{kn'\alpha l_2'}(r_1)dr_1\,, \tag{4.8b}$$

where the coefficients f_β and g_β,

$$f_\beta(l_1l_2,l_1'l_2';L)=\langle l_1l_2L\,|\,P_\beta(\hat{r}_1\cdot\hat{r}_2)\,|\,l_1'l_2'L\rangle \tag{4.9a}$$

and

$$g_\beta(l_1l_2,l_1'l_2';L)=(-)^{l_1+l_2-L}\langle l_1l_2L\,|\,P_\beta(\hat{r}_1\cdot\hat{r}_2)\,|\,l_2'l_1'L\rangle\,, \tag{4.9b}$$

are tabulated by Percival and Seaton.[13] Note that Eqs. (4.6) are not simply the usual set of coupled equations with the $1s$ term omitted, since in Eq. (4.6) the ϕ's are constrained to be orthogonal to the $1s$ state as required by Eq. (4.3).

We confine our treatment to within the $2s-2p$ close-coupling approximation[2] and consider the case where the (e,H) system has zero total angular momentum (i.e., $L=M=0$). In this case, $Q\Phi_\alpha$ becomes

$$Q\Phi_\alpha=\frac{(r_1,r_2)^{-1}}{4\pi}\{[\chi_{20}(r_1)\phi_{k2\alpha0}(r_2)-\sqrt{3}\chi_{21}(r_1)\phi_{k2\alpha1}(r_2)\cos\theta_{12}]+(-)^S[1\leftrightarrow2]\}\,, \tag{4.10}$$

and Eq. (4.6) reduces to a pair of coupled equations

$$\left\{\frac{d^2}{dr_2^2}+k_{2\alpha}^2\right\}\phi_{k2\alpha0}(r_2)=2\sum_{(l_1',l_2')=(0,0)}^{(1,1)}\{V_{200}^{\ 2l_1'l_2'}(r_2)\phi_{k2\alpha l_2'}(r_2)+K_{200}^{\ 2l_1'l_2'}(r_2,r_1)\phi_{k2\alpha l_2'}(r_1)\}\,, \tag{4.11a}$$

$$\left\{\frac{d^2}{dr_2^2}-\frac{2}{r_2^2}+k_{2\alpha}^2\right\}\phi_{k2\alpha1}(r_2)=2\sum_{(l_1',l_2')=(0,0)}^{(1,1)}\{V_{211}^{\ 2l_1'l_2'}(r_2)\phi_{k2\alpha l_2'}(r_2)+K_{211}^{\ 2l_1'l_2'}(r_2,r_1)\phi_{k2\alpha l_2'}(r_1)\}\,. \tag{4.11b}$$

It can be shown, in matrix notation, that Eq. (4.11) asymptotically becomes

$$\left\{\frac{d^2}{dr^2}+k_{2\alpha}^2\right\}\mathbf{\Phi}=\frac{\mathbf{A}}{r^2}\mathbf{\Phi}\,, \tag{4.12}$$

where $\mathbf{\Phi}$ is a unicolumnar matrix $\mathbf{A}$ is a square matrix:

$$\mathbf{\Phi}=\begin{pmatrix}\phi_{k2\alpha0}\\ \phi_{k2\alpha1}\end{pmatrix},\quad \mathbf{A}=\begin{pmatrix}0 & 6\\ 6 & 2\end{pmatrix}. \tag{4.13}$$

Equation (4.12) can be decoupled by a transformation $\mathbf{B}$ which diagonalizes matrix $\mathbf{A}$. The appropriate transformation is

$$\mathbf{B}=\begin{pmatrix}1 & 1\\ \frac{1}{6}(1-\sqrt{37}) & \frac{1}{6}(1+\sqrt{37})\end{pmatrix}. \tag{4.14}$$

Thus, one obtains the decoupled equations[4]

$$\left\{\frac{d^2}{dr^2}+k_{2\alpha}^2-\frac{1-\sqrt{37}}{r^2}\right\}\xi_\alpha(r)=0\,, \tag{4.15a}$$

$$\left\{\frac{d^2}{dr^2}+k_{2\alpha}^2-\frac{1+\sqrt{37}}{r^2}\right\}\eta_\alpha(r)=0\,, \tag{4.15b}$$

with

$$\begin{pmatrix}\xi_\alpha\\ \eta_\alpha\end{pmatrix}=\mathbf{B}^{-1}\mathbf{\Phi}\,,$$
$$\mathbf{B}^{-1}=(2\sqrt{37})^{-1}\begin{pmatrix}1+\sqrt{37} & -6\\ -1+\sqrt{37} & 6\end{pmatrix}. \tag{4.16}$$

We observe that Eq. (4.15b) has no bound-state solution and that Eq. (4.15b) has an infinite number of bound-state solutions resulting from the attractive dipole potential generated by the $2s-2p$ degenerate channels. The latter solutions do not require details

[13] I. C. Percival and M. J. Seaton, Proc. Cambridge Phil. Soc. 53, 654 (1957).

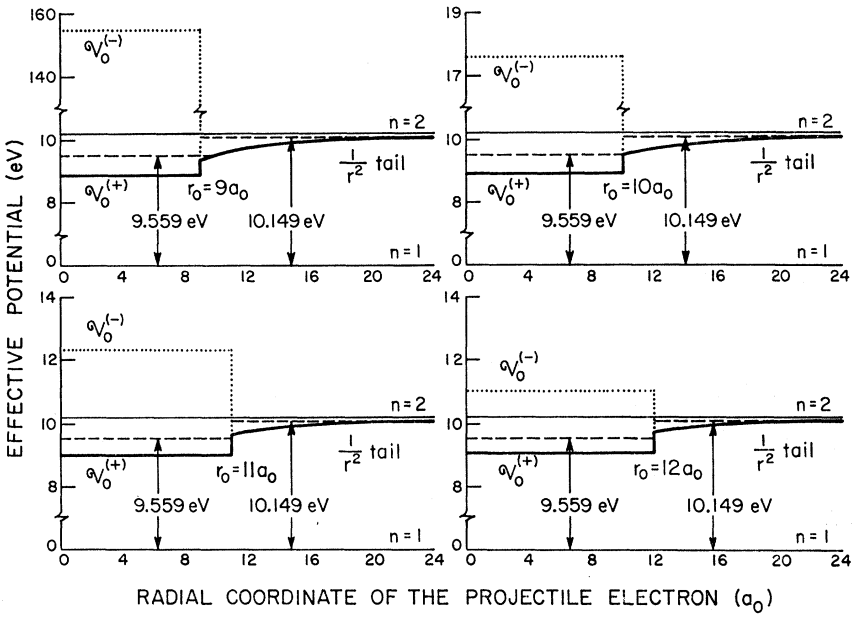

FIG. 1. The effective potential for a projectile electron in the excited $2s$-$2p$ degenerate field of a target hydrogen atom.

of the potential at small distances, provided it is not too singular at the origin.

At small distances, Eqs. (4.11a) and (4.11b) can no longer be decoupled by a linear transformation. One may, however, define a nonlocal optical potential[14] so that Eq. (4.11) is decoupled all the way to the origin. We assume that this nonlocal optical potential may be approximated by a local potential.[15] In view of these observations, we select for the effective potential $\mathcal{U}$ of the wave function ξ_α, a radius r_0 such that in the external region (i.e., $r\geq r_0$) the effective potential is given by the dipole term $-\frac{1}{2}(\sqrt{37}-1)/r^2$ and such that in the internal region (i.e., $r\leq r_0$) the effective potential is given by a constant $\mathcal{U}_0^{(\pm)}$ (Fig. 1). Thus, the approximate equation for ξ_α takes the form

$$\{d^2/dr^2+k_{2\alpha}{}^2-2\mathcal{U}^{(\pm)}(r)\}\xi_\alpha{}^{(\pm)}(r)=0, \quad (4.17)$$

with

$$\mathcal{U}^{(\pm)}(r)=\mathcal{U}_0{}^{(\pm)}, \qquad r\leq r_0 \quad (4.18a)$$

$$\mathcal{U}^{(\pm)}(r)=\lambda(\lambda+1)/2r^2, \qquad r\geq r_0 \quad (4.18b)$$

where

$$\lambda=-\tfrac{1}{2}+i(\sqrt{37}-5/4)^{1/2} \quad \text{and} \quad \lambda(\lambda+1)=-(\sqrt{37}-1).$$

Since the exchange terms vanish exponentially and do not contribute to the asymptotical potential, the dipole potential $\frac{1}{2}\lambda(\lambda+1)/r^2$ holds for both singlet and triplet states with $L=M=0$. At small distances, the exchange terms become significant and cause the potential to split according to the spin symmetry of the system (Fig. 1). We notice that for the triplet case the effective potential becomes repulsive in the internal region. This is because of the centrifugal barrier associated with the p-electron, since in the triplet case the $2p$-orbital is always occupied. To account for the spin symmetry, the potentials in Eq. (4.17) are labeled with the superscripts (+) and (−) corresponding to singlet and triplet states (*i.e.*, $S=0$, $S=1$), respectively. Thus, this permits us to approximate $\phi_{k_{2\alpha}0}$ and $\phi_{k_{2\alpha}1}$ in Eq. (4.10) as [see Eqs. (4.13) and (4.16)]

$$\phi_{k_{2\alpha}0}(r)=\xi_\alpha(r), \quad \phi_{k_{2\alpha}1}(r)=\tfrac{1}{6}(1-\sqrt{37})\xi_\alpha(r) \quad (4.19)$$

with appropriate spin symmetry. In writing Eq. (4.19), we have taken $\eta_\alpha=0$, since there is no bound-state solution for Eq. (4.15b). The well depth $\mathcal{U}_0{}^{(\pm)}$ and well width r_0 of the constant potential are chosen so that the lowest eigenvalues (for both the singlet and triplet states) match, respectively, that calculated by O'Malley and Geltman[5] (Fig. 1).

V. CALCULATION OF THE LEVEL POSITION

Wave functions $\xi_\alpha(r)$ are obtained by solving Eq. (4.17) for solutions which are bounded everywhere and decay exponentially at infinity, In view of the boundary conditions, the unnormalized wave functions ξ_α take the form

$$\xi_\alpha{}^{(\pm)}(r)=\sin(\kappa_\alpha{}^{(\pm)}r), \quad r\leq r_0$$
$$=a(\kappa_\alpha{}^{(\pm)},|k_{2\alpha}|r_0)r^{1/2}H_{i\lambda_0}{}^{(1)}(i|k_{2\alpha}|r), \quad r\geq r_0 \quad (5.1)$$

[14] M. Mittleman, Ann. Phys. (N. Y.) **14**, 94 (1961); B. A. Lippmann, M. Mittleman, and K. M. Watson, Phys. Rev. **116**, 920 (1959).

[15] It is obvious that at configuration space close to the nucleus the centrifugal barrier associated with the p electron becomes dominating and gives rise to an infinite potential wall. This may seriously limit our assumptions for approximating the nonlocal optical potential by a local potential. This difficulty is, however, partially removed by the fact that the compound wave functions extend very far in configuration space (Figs. 3 and 4) because of the long-range nature of the supporting potential, and by the fact that they are not strongly dependent on regions close to the nucleus. This is particularly so for higher members of the compound states.

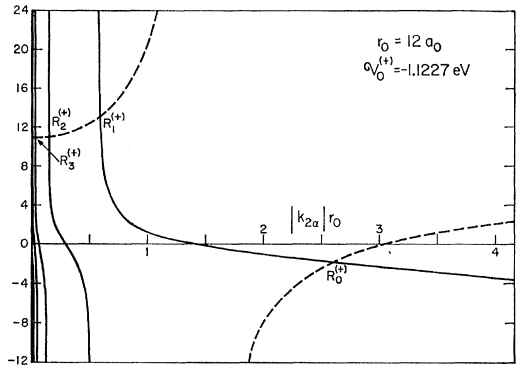

FIG. 2. Dispersion relations for the singlet compound-state wave function of the projectile electron [Eq. (5.8)]. The dashed and solid curves are, respectively, the values (multiplied by r_0) of the left-hand and right-hand sides of Eq. (5.8) as a function of $|k_{2\alpha}|r_0$. The parameters r_0 and $v_0^{(+)}$ are chosen so that the lowest root $R_0^{(+)}$ appears at $|k_{2\alpha}|=0.217696$ corresponding to $\varepsilon_0^{(+)}=9.559$ eV.

where

$$\kappa_\alpha^{(\pm)}=i\{2v_0^{(\pm)}+|k_{2\alpha}|^2\}^{1/2},$$
$$\lambda_0=-i(\lambda+\tfrac{1}{2})=(\sqrt{37}-5/4)^{1/2},$$

where a is a matching constant, and where the $H_{i\lambda}^{(1)}$'s are the Hankel functions of the first kind having the integral representation [Appendix B, Eq. (B3)]

$$H_{i\lambda_0}^{(1)}(i|k_{2\alpha}|r)$$
$$=\frac{2e^{\frac{1}{2}\pi\lambda_0}}{i\pi}\int_0^\infty e^{-|k_{2\alpha}|r\cosh(z)}\cos(\lambda_0 z)dz. \quad (5.2)$$

This is the expression used for numerical calculation of the Hankel function. Since the single-particle compound wave function $\phi_{\nu\alpha}(\mathbf{r})$ defined by the projection operator [see Eq. (4.3)] contains no ground-target-state component, we must require, in view of Eqs. (4.5) and (4.19), the $\xi_\alpha^{(\pm)}$'s to be orthogonal to $\chi_{10}(r)$,[16] i.e.,

$$\int_0^\infty \xi_\alpha^{(\pm)}(r)\chi_{10}(r)dr=0. \quad (5.3)$$

This implies that the expression for the $\xi_\alpha^{(\pm)}$'s given by Eq. (5.1) must be modified so that Eq. (5.3) is satisfied.

[16] Actually, the orthogonal condition between the ground target state and the single-particle compound wave function $\phi_{\nu\alpha}(\mathbf{r})$ of a p electron is automatically satisfied for $L=0$ due to the angular parts of the wave functions. Thus, the orthogonal restriction between the radial parts of the wave function

$$\int\phi_{k_{2\alpha l}}(r)\chi_{10}(\mathbf{r})dr=0$$

is not at all necessary. However, because of our approximation of the effective potential in the internal region $r\leq r_0$, we obtain, for both $\phi_{k_{2\alpha 0}}$ and $\phi_{k_{2\alpha 1}}$, the linear dependence on $\xi_\alpha(r)$ [Eq. (4.19)]. This leads to the curious orthogonal restriction on $\phi_{k_{2\alpha 1}}$ in the equation above as a consequence of Eqs. (4.19) and (4.22). This, however, will not strongly effect the properties of the compound states (footnote 15).

This leads to the expression

$$\xi_\alpha^{(\pm)}(r)=\sin(\kappa_\alpha^{(\pm)}r)-(b_1/c_1)\chi_{10}(r), \quad r\leq r_0$$
$$=a\{r^{1/2}H_{i\lambda_0}^{(1)}(i|k_{2\alpha}|r)-(b_2/c_2)\chi_{10}(r)\}, \quad r\geq r_0 \quad (5.4)$$

with

$$a=\frac{\sin(\kappa_\alpha^{(\pm)}r_0)-(b_1/c_1)\chi_{10}(r_0)}{r_0^{1/2}H_{i\lambda_0}^{(1)}(i|k_{2\alpha}|r_0)-(b_2/c_2)\chi_{10}(r_0)}, \quad (5.5)$$

$$b_1=\int_0^{r_0}\sin(\kappa_\alpha^{(\pm)}r)\chi_{10}(r)dr,$$

$$b_2=\int_{r_0}^\infty r^{1/2}H_{i\lambda_0}^{(1)}(i|K_{2\alpha}|r)\chi_{10}(r)dr, \quad (5.6)$$

$$c_1=\int_0^{r_0}|\chi_{10}(r)|^2dr,$$

$$c_2=\int_{r_0}^\infty|\chi_{10}(r)|^2dr, \quad (5.7)$$

where (c_1+c_2) is of course equal to unity. It is worth while to mention that, for most r_0 of interest, the term $(b_2/c_2)\chi_{10}(r)$ in Eq. (5.4) is very small for $r\geq r_0$ and can be neglected.

The continuity condition of the logarithmic derivatives of the wave function at $r=r_0$ requires

$$\left\{\frac{\partial}{\partial r}\ln[\sin(\kappa_\alpha^{(\pm)}r)-(b_1/c_1)\chi_{10}(r)]\right\}_{r=r_0}$$
$$=\left\{\frac{\partial}{\partial r}\ln[r^{1/2}H_{i\lambda_0}^{(1)}(i|k_{2\alpha}|r)-(b_2/c_2)\chi_{10}(r)]\right\}_{r=r_0} \quad (5.8)$$

which provides us with information concerning the resonance energies. In Figs. 2 and 3, we plot both sides

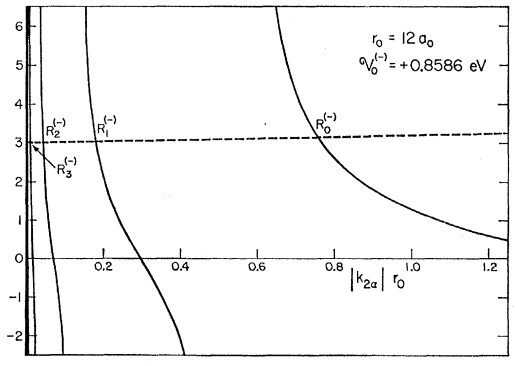

FIG. 3. Dispersion relations for the triplet compound-state wave functions of the projectile electron [Eq. (5.8)]. The dashed and solid curves are, respectively, the values (multiplied by r_0) of the left-hand and right-hand sides of Eq. (5.8) as a function of $|k_{2\alpha}|r_0$. The parameters r_0 and $v_0^{(-)}$ are chosen so that the lowest root $R_0^{(-)}$ appears at $|k_{2\alpha}|=0.063437$ corresponding to $\varepsilon_0^{(-)}=10.149$ eV.

of the dispersion relation as functions of $|k_{2\alpha}|r_0$ for singlet and triplet cases, respectively. The solutions of Eq. (4.17) are related to the corresponding roots in Eq. (5.8) as labeled by $R_\alpha^{(\pm)}$ with $\alpha=0, 1, 2, \cdots$ in Figs. 2 and 3. Thus, the energies of the compound states take the expression

$$\mathcal{E}_\alpha^{(\pm)}=\{\epsilon_2-\tfrac{1}{2}|k_{2\alpha}|^2\}=-\{\tfrac{1}{8}+\tfrac{1}{2}[R_\alpha^{(\pm)}/r_0]^2\}. \quad (5.9)$$

For each given r_0, the potentials in $\kappa_\alpha^{(\pm)}$ (i.e., $\mathcal{V}_0^{(+)}$ and $\mathcal{V}_0^{(-)}$ for the singlet and triplet spin multiplicities) are chosen so that the lowest singlet and triplet states appear, respectively, at $\mathcal{E}_0^{(+)}=9.559$ eV and $\mathcal{E}_0^{(-)}=10.149$ eV above the ground state of the target hydrogen. Although these values are the up bounds to the true quasistationary representations of the two lowest resonance energies, they nevertheless are the best available approximate values for Eq. (4.1) without the energy shift included [see Eq. (2.20)].

In Table I, the calculated energy levels of the first four compound states are tabulated for several chosen values of r_0 ($9\leq r_0\leq 12$). For comparison the results of O'Malley and Geltman,[5] of Temkin and Walker,[17] and of Burke and Taylor[18] are also included in Table I. We observe that for triplet states the calculated results are almost independent of the joining radius, indicating that these states are primarily supported by the $1/r^2$ potential tail. For singlet states, dependence of the first few energy levels on the joining radius is observed. This dependence is, however, not at all strong as can be seen in Table II, where we have tabulated the calculated singlet-state energy levels for several additional values of r_0 chosen closer to the nucleus. From Table II, it is observed that at $r_0=7a_0$ we obtain lowest values for both the singlet $\alpha=1$ and 2 states. Although the qualitative lowering of the energy levels is desirable, it is, however, doubtful if the lowering has any quantitative meaning, since the single-particle Schrödinger equation (4.17) is an approximate representation of Eq. (4.1). We choose $r_0=12a_0$ as the favorable joining radius since it closely reproduces the $\alpha=1$ values of O'Malley and Geltman for both the singlet and triplet $L=0$ states.

Returning now to Figs. 2 and 3, we observe that as the incident electron energy approaches the $n=2$ excitation threshold of the target hydrogen, the left-hand side of Eq. (5.8) tends to a constant for either singlet or triplet spin multiplicities of the system; and the right-hand side oscillates with increasing rapidity as a function of energy. Since the argument $|k_{2\alpha}|r_0$ of the Hankel function becomes increasingly small at these energies, we may replace the logarithmic derivative of the Hankel function in the right-hand side of Eq. (5.8) by its small-argument expression[17] [Appendix B, Eq. (B8)]. The dispersion relation [Eq. (5.8)] near

TABLE I. Level positions[a] of the ^1S and ^3S auto-ionization states of H^-.

Symmetry	Source[b]	$\mathcal{E}_0^{(\pm)}$	$\mathcal{E}_1^{(\pm)}$	$\mathcal{E}_2^{(\pm)}$	$\mathcal{E}_3^{(\pm)}$
^1S	$r_0=9$, $\mathcal{V}_0^{(+)}=-1.3182$	9.559	10.1646	10.2015	10.2036
	$r_0=10$, $\mathcal{V}_0^{(+)}=-1.2456$	9.559	10.1665	10.2016	10.2036
	$r_0=11$, $\mathcal{V}_0^{(+)}=-1.1801$	9.559	10.1685	10.2017	10.2036
	$r_0=12$, $\mathcal{V}_0^{(+)}=-1.1227$	9.559	10.1701	10.2018	10.2036
	O'MALLEY-Geltman[c]	9.559	10.178	···	···
	Temkin-Walker[d]	9.559	10.1668	10.2016	···
	Burke-Taylor[e]	9.560	10.1780	···	···
^3S	$r_0=9$, $\mathcal{V}_0^{(-)}=142.93$	10.149	10.2007	10.2036	10.2037
	$r_0=10$, $\mathcal{V}_0^{(-)}=7.4521$	10.149	10.2007	10.2036	10.2037
	$r_0=11$, $\mathcal{V}_0^{(-)}=2.1187$	10.149	10.2007	10.2036	10.2037
	$r_0=12$, $\mathcal{V}_0^{(-)}=0.8586$	10.149	10.2007	10.2036	10.2037
	O'Malley-Geltman[c]	10.149	10.202	···	···
	Temkin-Walker[d]	10.149	10.2006	10.2036	···
	Burke-Taylor[e]	10.1497	···	···	···

[a] In eV above the ground state of hydrogen atom (1 a.u. =27.21 eV).
[b] Joining radius in a_0 and potential in eV with the zero level set at the $n=2$ threshold of the hydrogen atom.
[c] Reference 5.
[d] Reference 17.
[e] Reference 18.

the threshold then takes the approximation

$$\lambda_0\cot[\lambda_0\ln(\tfrac{1}{2}|k_{2\alpha}|r_0)-\delta_{\lambda_0}(0)]+\tfrac{1}{2}=10.9151 \text{ (singlet)},$$
$$=3.02934 \text{ (triplet)}. \quad (5.10)$$

Solving Eq. (5.10) for $|k_{2\alpha}|$, we obtain to a good approximation the energy levels of the compound states near the threshold (relative to the ground state of the target hydrogen)

$$\mathcal{E}_\alpha^{(+)}\cong\tfrac{3}{8}-0.0216e^{-(2\pi/\lambda_0)\alpha}, \quad \alpha>2$$
$$\mathcal{E}_\alpha^{(-)}\cong\tfrac{3}{8}-0.0020e^{-(2\pi/\lambda_0)\alpha}, \quad \alpha>1. \quad (5.11)$$

Each oscillation in the right-hand side of Eq. (5.8) corresponds to a compound state approximated by Eq. (5.11).

The corresponding wave functions ξ_α so obtained extend very far in configuration space away from the target. Figures 4 and 5 exhibit the first few members of such wave functions (unnormalized) for the singlet and triplet states, respectively. The range parameters for these wave functions are found to be increasing exponentially as a function of α. This is a consequence of a long-range potential. Since wave functions ξ_α are related

TABLE II. Dependence of the level positions[a] on joining radius for the ^1S auto-ionization states of H^-.

Source[b]	$\mathcal{E}_0^{(+)}$	$\mathcal{E}_1^{(+)}$	$\mathcal{E}_2^{(+)}$	$\mathcal{E}_3^{(+)}$
$r_0=5$, $\mathcal{V}_0^{(+)}=-1.1535$	9.559	10.1644	10.2015	10.2036
$r_0=6$, $\mathcal{V}_0^{(+)}=-1.4463$	9.559	10.1625	10.2014	10.2036
$r_0=7$, $\mathcal{V}_0^{(+)}=-1.4537$	9.559	10.1620	10.2013	10.2036
$r_0=8$, $\mathcal{V}_0^{(+)}=-1.3930$	9.559	10.1629	10.2014	10.2036
O'Malley-Geltman[c]	9.559	10.178	···	···
Temkin-Walker[d]	9.559	10.1668	10.2016	···
Burke-Taylor[e]	9.560	10.1780	···	···

[a] In eV above the ground state of hydrogen atom (1 a.u. =27.21 eV).
[b] Joining radius in a_0 and potential in eV with the zero level set at the $n=2$ threshold of the hydrogen atom.
[c] Reference 5.
[d] Reference 17.
[e] Reference 18.

[17] A. Temkin and J. F. Walker, Phys. Rev. **140**, A1520 (1965).
[18] P. G. Burke and A. J. Taylor, Proc. Phys. Soc. (London) **88**, 549 (1966).

TABLE III. Level widths of the ^1S and ^3S auto-ionization states of H^-.

Symmetry	Source	$\Gamma_0^{(\pm)}$ (eV)	$\Gamma_1^{(\pm)}$ (eV)	$\Gamma_2^{(\pm)}$ (eV)	$\Gamma_3^{(\pm)}$ (eV)
^1S	Sine function[a]	0.0506	0.00645	3.94×10^{-4}	2.27×10^{-5}
	Static exchange[b]	0.041	0.00218	1.26×10^{-4}	7.22×10^{-6}
	Close-coupling[c,d]	0.109	0.0024	...	...
	Correlation[d]	0.0475	0.00219	...	...
	Experiment[e]	0.043 ± 0.006			
^3S	Sine function[a]	0.522×10^{-4}	3.37×10^{-6}	1.95×10^{-7}	1.13×10^{-8}
	Static exchange[b]	0.201×10^{-4}	1.18×10^{-6}	6.81×10^{-8}	3.92×10^{-9}
	Close-coupling[c,d]	0.189×10^{-4}	...	...	...
	Correlation[d]	0.206×10^{-4}	...	...	...

[a] Widths calculated from Eq. (6.1) using sine function approximation [Eq. (6.8)] for the single-particle channel wave function and approximate wave function (5.4) for the single-particle compound wave function with $r_0=12a_0$, $\mathcal{V}_0^{(+)}=-1.1227$ eV, and $\mathcal{V}_0^{(-)}=0.8586$ eV.
[b] Widths calculated from Eq. (6.1) using static-exchange approximation [Eq. (3.10)] for the single-particle channel wave function and approximate wave function (5.4) for the single-particle compound wave function with $r_0=12a_0$, $\mathcal{V}_0^{(+)}=-1.1227$ eV, and $\mathcal{V}_0^{(-)}=0.8586$ eV.
[c] $1s$-$2s$-$2p$ close coupling (Ref. 2).
[d] $1s$-$2s$-$2p$ close coupling with 16 correlation functions (Ref. 18).
[e] Reference 8.

to the radial parts of the single-particle compound wave function $\phi_{k_{2\alpha}l_j}(r_j)$ [Eq. (4.19)], the importance of the long-range potential is obvious. This observation demonstrates clearly for long-range potentials the shortcomings of formalism involving the concept of channel radius outside of which the incident particle is treated as free. This nonlocalized nature of the wave function may possibly constitute the reason why Burke and Schey[2] had to carry their close-coupling calculation as far as $r\simeq30a_0$ in configuration space in order to obtain convergences for the singlet $\alpha=0$ state when $2s-2p$ states are included.

VI. CALCULATION OF THE LEVEL WIDTH

The expression for the width is given by Eq. (2.24). When the expressions for $P\psi$ and $Q\Phi_\alpha$ given by Eqs. (3.3) and (4.2), respectively, are utilized, the expression for the width may be rewritten as

$$\Gamma_\alpha^{(\pm)}=8k_f\left|\gamma_{\rm dt}^{(\alpha)}\pm\gamma_{\rm ex}^{(\alpha)}\right|^2, \tag{6.1}$$

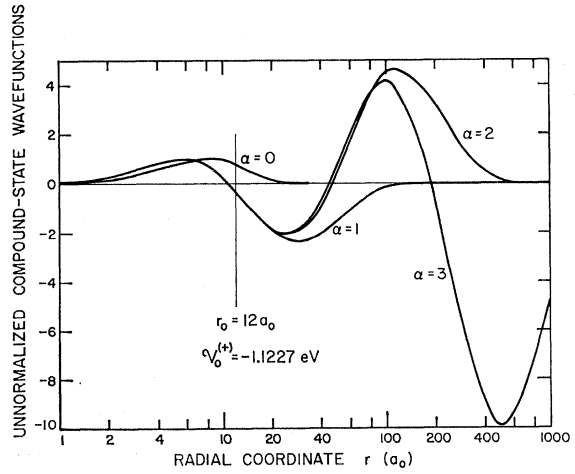

FIG. 4. First four members of the unnormalized wave functions $\xi_\alpha^{(+)}(r)$ [Eq. (5.4)] for singlet-spin multiplicity. These functions are related to the radial parts $[\phi_{k2\alpha0}(r)$ and $\phi_{k2\alpha1}(r)]$ of the single-particle compound wave functions $\phi_{\nu\alpha}(\mathbf{r})$ as follows: $\phi_{k2\alpha0}(r)=\xi_\alpha^{(+)}(r)$ for $n=2s$ and $\phi_{k2\alpha1}(r)=[1-\sqrt{37})/6]\xi_\alpha^{(+)}(r)$ for $n=2p$.

with

$$\gamma_{\rm dt}^{(\alpha)}=\sum_{\nu\neq1}\langle v_1(\mathbf{r}_2)\chi_1(\mathbf{r}_1)\,|\,V_0(\mathbf{r}_1,\mathbf{r}_2)\,|\,\chi_\nu(\mathbf{r}_1)\phi_{\nu\alpha}(\mathbf{r}_2)\rangle, \tag{6.2a}$$

$$\gamma_{\rm ex}^{(\alpha)}=\sum_{\nu\neq1}\langle v_1(\mathbf{r}_1)\chi_1(\mathbf{r}_2)\,|\,V_0(\mathbf{r}_1,\mathbf{r}_2)\,|\,\chi_\nu(\mathbf{r}_1)\phi_{\nu\alpha}(\mathbf{r}_2)\rangle, \tag{6.2b}$$

where the superscripts + and − on Γ_α indicate singlet and triplet states (i.e., $S=0$, and $S=1$), respectively. The first term $\gamma_{\rm dt}^{(\alpha)}$ in Eq. (6.1) gives the direct contribution to the width, and the second term $\gamma_{\rm ex}^{(\alpha)}$ gives the exchange contribution. After we decouple the angular states by using Eqs. (3.8) and (4.5), the γ's take the form

$$\gamma_{\rm dt}^{(\alpha)}=\sum_{\substack{n\neq1\\ \beta,l_1,l_2,l_2'}}f_\beta(0l_2',l_1l_2;\,L)\int_0^\infty\!\!\int v_{k1l_2}(r_2)\chi_{10}(r_1)\times\frac{r_<^\beta}{r_>^{\beta+1}}\chi_{nl_1}(r_1)\phi_{kn\alpha l_2}(r_2)dr_1dr_2, \tag{6.3a}$$

$$\gamma_{\rm ex}^{(\alpha)}=\sum_{\substack{n\neq1\\ \beta,l_1,l_2,l_2'}}g_\beta(0l_2',l_1l_2;\,L)\int_0^\infty\!\!\int v_{k1l_2}(r_1)\chi_{10}(r_2)\times\frac{r_<^\beta}{r_>^{\beta+1}}\chi_{nl_1}(r_1)\phi_{kn\alpha l_2}(r_2)dr_1dr_2, \tag{6.3b}$$

where the f's and g's are given by Eq. (4.9).

Equations (6.3a) and (6.3b) in the $2s-2p$ strong-coupling approximation reduce to the following equa-

TABLE IV. Dependence of the ^1S auto-ionization level widths[a] of H^- on joining radius.

	Source[b]	$\Gamma_0^{(+)}$	$\Gamma_1^{(+)}$	$\Gamma_2^{(+)}$	$\Gamma_3^{(+)}$
$r_0=7$,	$\mathcal{V}_0^{(+)}=-1.4537$	0.0822	0.01002	5.726×10^{-4}	3.340×10^{-5}
$r_0=10$,	$\mathcal{V}_0^{(+)}=-1.2456$	0.0633	0.00726	4.303×10^{-4}	2.471×10^{-5}
$r_0=12$,	$\mathcal{V}_0^{(+)}=-1.1227$	0.0506	0.00645	3.935×10^{-4}	2.272×10^{-5}
Burke-Taylor[c]		0.0475	0.00219	...	...

[a] Width in eV calculated from Eq. (6.1) using sine function approximation [Eq. (6.8)] for the single-particle channel wave function.
[b] Joining radius in a_0 and potential in eV with zero level set at $n=2$ threshold of the hydrogen atom.
[c] Reference 18.

TABLE V. Compound-state dependence of the direct and exchange contributions to the width and normalization constant.

Symmetry	Source	States	$\gamma_\alpha^{(\pm)}$ (eV)[a]	$N_{dt}^{(\alpha)}$ [b]	$N_{ex}^{(\alpha)}$ [c]
^1S	$r_0=12a_0$, $v_0^{(+)}=-1.1227$ eV	$\alpha=0$	0.275	1.477×10^1	8.472
		$\alpha=1$	0.201	3.096×10^2	6.821
		$\alpha=2$	0.193	5.273×10^3	6.627
		$\alpha=3$	0.192	9.165×10^4	6.616
^3S	$r_0=12a_0$, $v^{0(-)}=0.8580$ eV	$\alpha=0$	0.150	2.594×10^4	1.236×10^2
		$\alpha=1$	0.131	3.839×10^5	1.088×10^2
		$\alpha=2$	0.130	6.626×10^6	1.080×10^2
		$\alpha=3$	0.130	1.115×10^8	1.080×10^2

[a] Unnormalized matrix element for the width defined by Eq. (6.9).
[b] Direct contribution to the normalization constant for $Q\Phi_\alpha$ [Eq. (6.11)].
[c] Exchange contribution to the normalization constant for $Q\Phi_\alpha$ [Eq. (6.10)].

tions in the matrix notation:

$$\gamma_{dt}^{(\alpha)}=\langle v_{k_10}|\mathbf{V}|\mathbf{\Phi}\rangle, \tag{6.4a}$$

$$\gamma_{ex}^{(\alpha)}=\langle v_{k_10}|\mathbf{K}|\mathbf{\Phi}\rangle, \tag{6.4b}$$

where $\mathbf{V}$ and $\mathbf{K}$ are the row matrices

$$\mathbf{V}=(V_{100}{}^{200}V_{100}{}^{211}), \tag{6.5a}$$

$$\mathbf{K}=(K_{100}{}^{200}K_{100}{}^{211}) \tag{6.5b}$$

and the meaning of the matrix elements of $\mathbf{V}$ and $\mathbf{K}$ is clear from Eq. (4.8). The column matrix $\mathbf{\Phi}$ is given by Eqs. (4.13) and (4.19).

$$\mathbf{\Phi}=\begin{pmatrix}\xi_\alpha(r)\\ \frac{1}{6}(1-\sqrt{37})\xi_\alpha(r)\end{pmatrix}=\begin{pmatrix}1\\ \frac{1}{6}(1-\sqrt{37})\end{pmatrix}\xi_\alpha(r). \tag{6.6}$$

The wave functions $\xi_\alpha(r)$ obtained in Sec. IV must satisfy the relation

$$\frac{37-\sqrt{37}}{9}\langle\xi_\alpha^{(\pm)}(r)|\xi_\alpha^{(\pm)}(r)\rangle\pm2\left\{|\langle\xi_\alpha^{(\pm)}(r)|\chi_{20}(r)\rangle|^2+\frac{19-\sqrt{37}}{18}|\langle\xi_\alpha^{(\pm)}(r)|\chi_{21}(r)\rangle|^2\right\}=1, \tag{6.7}$$

so that $Q\Phi_\alpha$ as approximated by Eq. (4.10) is normalized to unity.

The width can now be estimated from Eq. (6.1) with the single-particle channel wave function $v_{k_10}(r)$ determined from Eq. (3.10) at $k_1=k_f$ with the electron wave number k_f in the exit channel corresponding to the resonance energies [i.e., at values of $E=\mathcal{E}_{2\alpha}$, $k_1{}^2=2(E-\epsilon_1)$]. The calculated widths are tabulated in Table III together with that calculated by Burke and Taylor.[18] Except for the lowest ^1S state, the agreement is reasonably good. For comparison, we also included in Table III, the measured value of the lowest ^1S resonance width and values for the widths derived by approximating the single-particle channel wave function by the simple sine function

$$v_{k_10}\cong k_1{}^{-1}\sin(k_1r). \tag{6.8}$$

Judging from the differences in calculated values for the width, it is apparent that the static-exchange distortion of the channel wave function is of importance. This suggests that width depends strongly on the channel wave function v_{k_10}. Thus one should really use more adequate solutions of Eq. (3.6) which may be obtained, for example, by the variational method.

We have also investigated in a limited sense the dependence of the level width on joining radius using approximation (6.8) for the channel wave functions. The results are summarized in Table IV. We notice that the dependence on r_0 for the level widths is similar to that for the level positions. The values of the width change moderately for $\alpha>1$. The width of the lowest state $\alpha=0$ which is supported largely by a potential in the interior region changes significantly. We expect that for states near the threshold the results for the width calculated using static-exchange approximation are, however, sufficiently reliable to draw some meaningful conclusions.

It is instructive to examine the unnormalized matrix elements for the widths which are defined as

$$\hat{\gamma}_\alpha^{(\pm)}=\{\gamma_{dt}^{(\alpha)}\pm\gamma_{ex}^{(\alpha)}\}^2\langle\Phi_\alpha|Q|\Phi_\alpha\rangle \tag{6.9}$$

with

$$\langle\Phi_\alpha|Q|\Phi_\alpha\rangle=2\{N_{dt}^{(\alpha)}\pm N_{ex}^{(\alpha)}\}, \tag{6.10}$$

where $N_{dt}^{(\alpha)}$ and $N_{ex}^{(\alpha)}$ are the direct and exchange contributions to the normalization constant for the

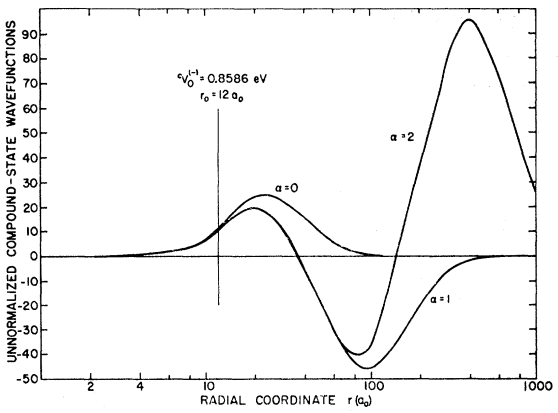

FIG. 5. First three members of the unnormalized wave functions $\xi_\alpha^{(-)}(r)$ [Eq. (5.4)] for triplet-spin multiplicity. These functions are related to the radial parts $[\phi_{k_2\alpha0}(r)$ and $\phi_{k_2\alpha1}(r)]$ of the single-particle compound wave functions $\phi_{\nu\alpha}(\mathbf{r})$ as follows: $\phi_{k_2\alpha0}(r)=\xi_\alpha^{(-)}(r)$ for $n=2s$ and $\phi_{k_2\alpha1}(r)=[(1-\sqrt{37})/6]\xi_\alpha^{(-)}(r)$ for $n=2p$.

compound state $Q\Phi_\alpha$. We tabulated, in Table V, the quantities $\hat{\gamma}_\alpha^{(\pm)}$, $N_{\rm dt}^{(\alpha)}$, and $N_{\rm ex}^{(\alpha)}$ as a function of α for $r_0=12a_0$. It is observed that as α becomes large (i.e., the level positions approach the $n=2$ excitation threshold), all the quantities stay approximately constant except for $N_{\rm dt}^{(\alpha)}$ which increases exponentially. This suggests that widths decrease exponentially with increasing α. The behavior of $\gamma^{(\alpha)}$, and $N_{\rm ex}^{(\alpha)}$ with increasing α can be understood from the fact that the wave functions of the higher members (large α) are almost identical within and near the domain of the target hydrogen [see Figs. 4 and 5].

The direct contribution to the normalization constant $N_{\rm dt}^{(\alpha)}$ may be explicitly written in terms of the Hankel function:

$$N_{\rm dt}^{(\alpha)}=\frac{37-\sqrt{37}}{18}\left\{\int_0^{r_0}|\sin(\kappa_\alpha^{(\pm)}r)-(b_1/c_1)\chi_{10}(r)|^2dr + |a(r_0)|^2\int_{r_0}^{\infty}|H_{i\lambda_0}^{(1)}(i|k_{2\alpha}|r)|^2rdr\right\}, \quad (6.11)$$

where a, b_1, and c_1 are defined in Eqs. (5.5) to (5.7). For small argument $|k_{2\alpha}|r\to 0$ (i.e., α becomes large), $N_{\rm dt}^{(\alpha)}$ takes the approximation [Appendix B, Eqs. (B9) and (B12)]

$$\begin{aligned}N_{\rm dt}^{(\alpha)}&\cong(1.75\times10^{1})e^{(2\pi/\lambda_0)\alpha}\ \text{(singlet states)},\\ &\cong(2.04\times10^{4})e^{(2\pi/\lambda_0)\alpha}\ \text{(triplet states)},\end{aligned} \quad (6.12)$$

where we have used the small-argument expressions for $|k_{2\alpha}|$ derived from Eq. (5.10). This permits us to write for the level widths near the threshold as (in atomic units)

$$\begin{aligned}\Gamma_\alpha^{(+)}&\cong\{1.397\times10^{-3}\}e^{-(2\pi/\lambda_0)\alpha},\\ \Gamma_\alpha^{(-)}&\cong\{7.387\times10^{-7}\}e^{-(2\pi/\lambda_0)\alpha}.\end{aligned} \quad (6.13)$$

We find therefore that widths, just like the spacings between their corresponding states, decrease exponentially near the threshold. It is then of interest to examine whether the series of singlet- and triplet-compound (auto-ionization) states just below the $n=2$ threshold are overlapping or isolated.

If we assume that the shifts in resonance energies due to the second part of Eq. (2.20) are negligibly small, it is then easy to show from Eq. (5.11) that the spacings between the compound states decrease exponentially as

$$\begin{aligned}\Delta\mathcal{E}_\alpha^{(+)}&=\tfrac{1}{2}|\mathcal{E}_{\alpha-1}^{(+)}-\mathcal{E}_{\alpha+1}^{(+)}|=0.1873e^{-(2\pi/\lambda_0)\alpha},\\ \Delta\mathcal{E}_\alpha^{(-)}&=\tfrac{1}{2}|\mathcal{E}_{\alpha-1}^{(-)}-\mathcal{E}_{\alpha+1}^{(-)}|=0.0173e^{-(2\pi/\lambda_0)\alpha}.\end{aligned} \quad (6.14)$$

Despite the fact that both the level widths and spacings decrease exponentially, their ratios for the singlet and triplet series, however, remain constant near the threshold:

$$\begin{aligned}\Gamma_\alpha^{(+)}/\Delta\mathcal{E}_\alpha^{(+)}&=7.46\times10^{-3},\\ \Gamma_\alpha^{(-)}/\Delta\mathcal{E}_\alpha^{(-)}&=4.27\times10^{-5}.\end{aligned} \quad (6.15)$$

Thus, it appears (because of the less-than-one ratios) that within our model neither the singlet nor the triplet series of the S auto-ionization states are overlapping near the threshold. The corresponding values for the width-spacing ratios obtained in sine-function approximation [Eq. (6.8)] for the singlet and triplet series are, respectively, 2.35×10^{-2} and 1.26×10^{-4} which are also less than 1.

The exponential formula [Eq. (6.13)] for the widths reproduces closely the calculated widths [Table III] for both the singlet and triplet series near the threshold. It is surprising that this formula also reproduces reasonably well the calculated widths for the $\alpha=0$ states. The only exception occurs in the sine approximation for the width of the lowest singlet state. The calculated width using the same sine function approximation is much greater (by a factor of approximately 2) than that predicted by the formula. This is due to the fortuitous absence of cancellation of the area spanned by the integral in the sine function approximation. As a result a better agreement with the experimental results is obtained.

VII. CALCULATION OF THE CROSS SECTION

The transition matrix $\mathcal{T}$ for the elastic scattering can be obtained from Eq. (2.25):

$$\mathcal{T}=\mathcal{T}_p+\sum_\alpha\Lambda_\alpha\langle p\psi^{(-)}|PHQ|Q\Phi_\alpha\rangle, \quad (7.1)$$

where $\mathcal{T}_p$ represents the potential scattering and the Λ_α's are the resonance structure functions satisfying Eq. (2.27). The cross section then takes the form

$$\sigma=\frac{1}{4\pi^2}\int\{\tfrac{1}{4}|\mathcal{T}^{(+)}|^2+\tfrac{3}{4}|\mathcal{T}^{(-)}|^2\}d\Omega, \quad (7.2)$$

where the superscripts (+) and (−) stand for the singlet- and triplet-spin multiplicities, respectively.

For the sake of clarity, we assume that at the energy region of our interest there is only one resonant state of significance for each spin multiplicity. Equation (7.1) then reduces to

$$\mathcal{T}^{(\pm)}=\mathcal{T}_p^{(\pm)}+\frac{|\gamma_\alpha^{(\pm)}|^2e^{2i\delta_0(\pm)}}{E-\mathcal{E}_\alpha'^{(\pm)}+\frac{1}{2}i\Gamma_\alpha^{(\pm)}} \quad (7.3)$$

with

$$\gamma_\alpha=\langle p\psi^{(-)}|PHQ|Q\Phi_\alpha\rangle, \quad (7.4)$$

where we have used Eqs. (2.17) to (2.21). By utilizing Eq. (2.24), the $\mathcal{T}$ matrix can be rewritten as

$$\mathcal{T}^{(\pm)}=\mathcal{T}_p^{(\pm)}+\frac{(\pi/k)\Gamma_\alpha^{(\pm)}e^{2i\delta_0(\pm)}}{E-\mathcal{E}_\alpha'^{(\pm)}+\frac{1}{2}i\Gamma_\alpha^{(\pm)}}. \quad (7.5)$$

From Eqs. (3.1) and (3.2) it is clear that the potential scattering comes from three sources, namely the static field of the target hydrogen, the exchange interaction

between the projectile and atomic electrons, and the polarization effects due to virtual excitation. In principle, the potential scattering can be obtained exactly by solving Eq. (2.18) [or Eq. (3.6)]. We then have, for the case $L=M=0$,

$$\mathcal{T}_p^{(\pm)} = -(2\pi/k)e^{i\delta_0{}'^{(\pm)}} \sin\delta_0^{(\pm)}, \tag{7.6}$$

where $\delta_0^{(\pm)}$ is the phase shift due to potential scattering. Substitution of Eq. (7.5) with $\mathcal{T}_p^{(\pm)}$ given by Eq. (7.6) into Eq. (7.2) yields, for the case $L=M=0$,

$$\sigma = \tfrac{1}{4}\sigma^{(+)} + \tfrac{3}{4}\sigma^{(-)}, \tag{7.7}$$

with

$$\sigma^{(\pm)} = \frac{4\pi}{k^2}\left| e^{i\delta_0^{(\pm)}} \sin\delta_0^{(\pm)} - \frac{\frac{1}{2}\Gamma^{(\pm)} e^{2i\delta_0^{(\pm)}}}{E - \mathcal{E}'^{(\pm)} + \frac{1}{2}i\Gamma^{(\pm)}}\right|^2$$

$$= \frac{4\pi}{k^2}\left\{ |\sin\delta_0^{(\pm)}|^2 + \frac{\frac{1}{4}[\Gamma^{(\pm)}]^2}{[E-\mathcal{E}'^{(\pm)}]^2 + \frac{1}{4}[\Gamma^{(\pm)}]^2} - 2\,\mathrm{Re}\left[\frac{\frac{1}{2}\Gamma^{(\pm)} \sin\delta_0^{(\pm)} e^{i\delta^{(\pm)}}}{E - \mathcal{E}'^{(\pm)} + \frac{1}{2}i\Gamma^{(\pm)}}\right]\right\}, \tag{7.8}$$

where the three terms in Eq. (7.8) are in order the potential, resonance, and interference contributions to the cross section.

Recently, the energy dependence of the scattered-electron current from hydrogen atoms has been measured.[6] The dependence exhibits the profile predicted by Burke and Schey.[2] It is therefore of interest to calculate the energy dependence of the interference between potential and resonance scatterings.[19] We have noted before (Sec. III) that potential scattering depends strongly on polarization effects of the nonlocal optical potential so that the phase shift obtained in the static-exchange approximation [Eqs. (3.10) to (3.13)] is not adequate for calculating $\mathcal{T}_p^{(\pm)}$ from Eq. (7.6). To be consistent with approximations being made in this study, we adopt the values of the phase shift calculated using the $1s-2s-2p$ close-coupling approximation[2,18] and subtract from it the resonance part of the phase shift. Hence, the potential-scattering phase shift is given by

$$\delta_0^{(\pm)} = \tilde{\delta}_0^{(\pm)} + \tan^{-1}\left\{\frac{\frac{1}{2}\tilde{\Gamma}^{(\pm)}}{E - \tilde{\mathcal{E}}^{(\pm)}}\right\}, \tag{7.9}$$

where $\tilde{\delta}_0^{(\pm)}$ is the total s-wave phase shift (i.e., the sum of potential and resonance phase shifts) and $\tilde{\Gamma}^{(\pm)}$ and $\tilde{\mathcal{E}}^{(\pm)}$ are the corresponding width and resonance energy calculated in the $1s-2s-2p$ close-coupling approximation.[2]

In Fig. 6 the interference contributions together with the potential and resonance contributions to the cross section are plotted for the $L=0$ elastic scattering with singlet- and triplet-spin multiplicities. The interference contributions to the cross section depend strongly on the width. For the singlet case, the interference contribution is not only significant, but it gives rise to the profile of the cross section. On the other hand, if the width is very narrow the structure due to the interference becomes difficult to observe as in the triplet case. The total partial cross section for $L=0$ elastic scattering is then obtained from Eq. (7.7) which exhibits the general profile predicted by Burke and Schey[2] and observed by McGowan *et al.*[6c,8,20] We have not carried our calculation higher in energy than that given in Fig. 6. Judging from the dependence of the interference and resonance contributions on the width, we expect that the lowest triplet p-resonance states and possibly the second singlet s-resonance state may also give rise to structures in the cross section which may be observable within the present experimental resolution.

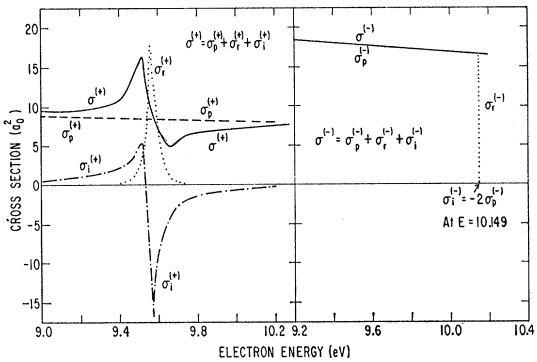

FIG. 6. Calculated potential, resonance, and interference contributions, which are denoted by σ_p, σ_r, and σ_i, respectively, to the cross section for s-wave electron scattering by hydrogen atoms.

VIII. DISCUSSION

The model study presented here is a convenient way of obtaining information concerning the resonance structure in electron scattering by hydrogen atoms without using elaborate computor calculations. Extension of the method used in the model study to resonance series other than the s-wave scattering or to resonances in excitation channels (or to other appropriate systems) is straightforward since, in general, the angular-degenerate coupled equations at the nth threshold can asymptotically reduce to [compare with Eq. (4.12)][21]

$$[d^2/dr^2 + k_{n\alpha}{}^2]\mathbf{\Phi}_n = (\mathbf{A}_n/r^2)\mathbf{\Phi}_n \tag{8.1}$$

where $\mathbf{A}_n$ can always be diagonalized by a transformation matrix $\mathbf{B}_n$. The projection operator discussed in Sec. II in this case must be modified appropriately to include more open channels.

[19] U. Fano, Phys. Rev. **124**, 1866 (1961).

[20] A more elaborate calculation of the cross-section profile was carried out by J. W. McGowan which include $L\neq 0$ scatterings. I am grateful to him for helpful discussions.

[21] P. G. Burke, Advan. Phys. **14**, 521 (1965); M. H. Mittleman, Phys. Rev. **147**, 73 (1966).

There are, however, a number of shortcomings in the model study which should be discussed. In Sec. VI, we have observed that the calculated values of the width depend strongly on the accuracy of the single-particle channel wave function being used. This then casts some doubt on the accuracy of the calculated width. Other than the limited encouragement found in the comparison of the calculated width with other approximate calculations (Table III), the question concerning the reliability of the static-exchange approximation [Eq. (3.10)] for the width is left unanswered. If an extensive calculation for the channel wave function is attempted from Eq. (3.6), the nonlocal optical potential must first be constructed explicitly. We then encounter a problem which is as elaborate as solving the coupled equations directly. This then defeats the purpose of such a model study. However, it is rather unlikely that the state-exchange approximation for the channel wave function will introduce significant errors which would mislead us in our conclusions for the resonances near the threshold. We also expect that level shifts [see Eq. (2.20)] are small and would not affect our conclusions.

If, in addition to the level position, an accurate value of the level width is utilized for the lowest state of a given resonance series, then an iteration procedure may be constructed so that a consistent set of joining radius and potential well may be determined. This may result in somewhat better values for the width. We are still facing the ambiguity of whether the joining radius and potential well so obtained are the properties of the approximate channel wave function being used in the calculation of the width. One may nevertheless improve the approximate procedure by constructing a more realistic interior potential for the projectile electron. An approximate interior (nonlocal) potential may be determined from a variational wave function $Q\Phi_\alpha^{(\mathrm{tr})}$ which is obtained from Eq. (4.4) by a constraint variational method. The trial variational wave function can be constructed in such a way[22] that its constituent single-particle compound wave function $\phi_{\nu\alpha}$ [see Eqs. (4.2) and (4.5)] asymptotically assume the appropriate expression given by Eq. (5.2).

Errors arising from the approximations being made in determining the single-particle compound wave function are believed to be small for $\alpha \geq 1$ states, since these wave functions not only yield the correct level positions but also possess the correct asymptotic expressions demanded by the appropriate r^{-2} long-range potential. The latter property of the wave function is of importance since for the calculation of width the electronic distribution at large r becomes very significant. For more complicated systems, the appropriate long-range potentials for the projectile electron are not usually available; it is then not possible to determine the desired asymptotical expressions for the compound wave functions. This method of course becomes useless. Note that the regular Q-space optimized variational wave function may yield sufficiently accurate quasi-stationary level positions. But it may not necessarily yield as accurate values for level width since the accuracy of the calculated width depends strongly on whether the variational wave function has the correct asymptotic electronic distributions. A double-perturbation method for such a case may be derived to improve systematically the calculation of the width.[22]

[22] J. C. Y. Chen, Bull. Am. Phys. Soc. **11**, 722 (1966).

ACKNOWLEDGMENTS

A major part of this work was done during the author's sojourn at the Department of Theoretical Physics, University of Manchester. He is grateful to Professor B. H. Flowers, F. R. S. for the hospitality extended to him by the Department. In particular, he wishes to thank Dr. A. Herzenberg and Dr. F. Mandl for their profitable suggestions and discussions. The author also wishes to acknowledge the generous assitance of Dr. J. W. Cooper in making the static-exchange wave functions available to him, and of Mrs. Joni Sue Lane in programming.

APPENDIX A: UNIQUENESS OF PARTICLE WAVE FUNCTIONS IN THE TARGET-STATE EXPANSION

The expansion[23] of a two-electron function $\Upsilon(\mathbf{r}_1,\mathbf{r}_2)$ which has a specified symmetry

$$\Upsilon(\mathbf{r}_1,\mathbf{r}_2)=(-)^S\Upsilon(\mathbf{r}_2,\mathbf{r}_1) \tag{A1}$$

and a specified angular momentum L but which is otherwise arbitrary can always be made in terms of a complete set of one-electron target states $\{\chi_\nu(\mathbf{r})\}$ so that

$$\Upsilon(\mathbf{r}_1,\mathbf{r}_2)=\sum_\nu \{\chi_\nu(\mathbf{r}_1)G_\nu(\mathbf{r}_2)+(-)^S\chi_\nu(\mathbf{r}_2)G_\nu(\mathbf{r}_1)\}. \tag{A2}$$

This expansion, however, does not define the particle wave functions $G_\nu(\mathbf{r})$ uniquely. This nonuniqueness has been pointed out and their effects on the absolute definition of the phase shift has been discussed.[10,24] Here we would like to investigate in details the extent of the nonuniqueness for $G_\nu(\mathbf{r})$.

Let us define in terms of $\Upsilon(\mathbf{r}_1,\mathbf{r}_2)$ and of target states the quantities $C_{\nu\nu'}$:

$$C_{\nu\nu'}=\langle\chi_\nu(\mathbf{r}_1)\chi_{\nu'}(\mathbf{r}_2)\,|\,\Upsilon(\mathbf{r}_1,\mathbf{r}_2)\rangle, \tag{A3}$$

which are obviously unique for a specified $\Upsilon(\mathbf{r}_1,\mathbf{r}_2)$, and satisfy the symmetry condition inferred from Eq. (A1)

$$C_{\nu\nu'}=(-)^SC_{\nu'\nu}. \tag{A4}$$

Now expanding the particle wave functions in terms of

[23] I am grateful to Dr. R. Phythian for his helpful discussions.
[24] A. Temkin, J. Math. Phys. **2**, 336 (1961).

the target states, we have

$$G_\nu(\mathbf{r})=\tfrac{1}{2}\sum_{\nu'}(C_{\nu\nu'}+D_{\nu\nu'})\chi_{\nu'}(\mathbf{r}), \tag{A5}$$

where the $D_{\nu\nu'}$'s are defined in terms of the inner products $\langle\chi_{\nu'}(\mathbf{r})|G_\nu(\mathbf{r})\rangle$

$$D_{\nu\nu'}=2\langle\chi_{\nu'}(\mathbf{r})|G_\nu(\mathbf{r})\rangle-C_{\nu\nu'}. \tag{A6}$$

Substituting $G_\nu(\mathbf{r})$ given by Eq. (A5) into Eq. (A2) and operating on the resultant equation by

$$\langle\chi_\nu(\mathbf{r}_1)\chi_{\nu'}(\mathbf{r}_2)|,$$

we obtain

$$\langle\chi_\nu(\mathbf{r}_1)\chi_{\nu'}(\mathbf{r}_2)|\ \Psi(\mathbf{r}_1,\mathbf{r}_2)\rangle=C_{\nu\nu'}+\tfrac{1}{2}\{D_{\nu\nu'}+(-)^S D_{\nu'\nu}\}. \tag{A7}$$

Comparison of Eq. (A7) with Eq. (A3) reveals that the $G_\nu(\mathbf{r})$'s are defined in Eq. (A2) within the ambiguity of $D_{\nu\nu'}$ which has the following symmetry:

$$D_{\nu\nu'}=(-)^{S+1}D_{\nu'\nu}. \tag{A8}$$

This ambiguity in $G_\nu(\mathbf{r})$ provides us with extra degrees of freedom for imposing further restrictions on the $G_\nu(\mathbf{r})$'s.

From Eq. (A5), we have

$$\langle\chi_\nu(\mathbf{r})|G_{\nu'}(\mathbf{r})\rangle=\tfrac{1}{2}\{C_{\nu'\nu}+D_{\nu'\nu}\}. \tag{A9}$$

Thus we may make the particle wave functions $G_\nu(\mathbf{r})$ orthogonal to the target states by appropriate choice of $D_{\nu'\nu}$ whenever it is allowed. For singlet states (i.e., $S=0$), we may choose (note $D_{\nu\nu}=0$)

$$D_{\nu\nu'}=C_{\nu'\nu},\quad \nu'>\nu \tag{A10}$$

and for triplet states (i.e., $S=1$), we may choose

$$D_{\nu'\nu}=C_{\nu\nu'},\quad \nu'\geq\nu \tag{A11}$$

so that the orthogonality conditions are satisfied.

For the projection operator P and Q with $P=P_1(\mathbf{r}_1)+P_1(\mathbf{r}_2)-P_1(\mathbf{r}_1)P_1(\mathbf{r}_2)$, $Q=1-P$ and $P_1(\mathbf{r})=|\chi_1(\mathbf{r})\rangle\langle\chi_1(\mathbf{r})|$, it is most convenient to define the $G_\nu(\mathbf{r})$'s as

$$G_\nu(\mathbf{r}_j)=\tfrac{1}{2}[1+\delta_{\nu 1}-P_1(r_j)]\langle\chi_\nu(\mathbf{r}_i)|\Upsilon(\mathbf{r}_i,\mathbf{r}_j)\rangle. \tag{A12}$$

In terms of the $C_{\nu\nu'}$'s, Eq. (A12) becomes

$$G_\nu(\mathbf{r}_j)=\tfrac{1}{2}(1+\delta_{\nu 1})\sum_{\nu'}C_{\nu\nu'}\chi_{\nu'}(\mathbf{r}_j)-\tfrac{1}{2}C_{\nu 1}\chi_1(\mathbf{r}_j). \tag{A13}$$

By comparison of Eq. (A13) with Eq. (A5), we may summarize the choice of $D_{\nu\nu'}$ in our definition of G_ν [Eq. (A12)] by the matrix

$$\mathbf{D}=\begin{pmatrix} 0 & C_{12} & C_{13} & C_{14} & \cdots \\ -C_{21} & 0 & 0 & 0 & \cdots \\ -C_{31} & 0 & 0 & 0 & \cdots \\ -C_{41} & 0 & 0 & 0 & \cdots \\ \vdots & \vdots & \vdots & \vdots & \end{pmatrix}. \tag{A14}$$

This implies that the $D_{\nu\nu'}$ are chosen in such a way that the particle wave functions are orthogonal to the ground target state except for $G_1(\mathbf{r})$, i.e.,

$$\langle G_\nu(\mathbf{r})|\chi_1(\mathbf{r})\rangle=0,\quad \nu\neq 1. \tag{A15}$$

This is self-evident from our definition for the G_ν's [Eq. (A12)].

APPENDIX B: INTEGRAL REPRESENTATION AND EXTREME EXPRESSIONS FOR THE HANKEL FUNCTION

The Hankel function of the first kind $H_\beta^{(1)}(z)$ has the integral representation

$$H_\beta^{(1)}(z)=-\frac{1}{\pi}\int_{\mathfrak{L}}e^{-iz\sin\zeta+i\beta\zeta}d\zeta, \tag{B1}$$

where $\zeta=\zeta_1+i\zeta_2$, and the contour path $\mathfrak{L}$ is shown in Fig. 7(a). If we choose $\zeta_1'=-\frac{1}{2}\pi$, the contour path becomes that shown in Fig. 7(b), and the integral takes the expression

$$\begin{aligned}H_\beta^{(1)}(z)&=\frac{1}{i\pi}\int_{-\infty}^{\infty}e^{-iz\sin[-(\pi/2)+i\zeta_2]+i\beta[-(\pi/2)+i\zeta_2]}d\zeta_2\\&=\frac{e^{-i(\pi/2)\beta}}{i\pi}\int_{-\infty}^{\infty}e^{iz\cosh(\zeta_2)-\beta\zeta_2}d\zeta_2.\end{aligned} \tag{B2}$$

For the special case $\beta=i\lambda_0$ and $z=i|k_{2\alpha}|r$ appearing in Eq. (5.1), we then have[25]

$$\begin{aligned}H_{i\lambda_0}(i|k_{2\alpha}|r)&=\frac{e^{(\pi/2)\lambda_0}}{i\pi}\left\{\int_0^{\infty}e^{-|k_{2\alpha}|r\cosh(\zeta_2)-i\lambda_0\zeta_2}d\zeta_2\right.\\&\quad\left.+\int_0^{\infty}e^{-|k_{2\alpha}|r\cosh(\zeta_2)+i\lambda_0\zeta_2}d\zeta_2\right\}\\&=\frac{2e^{(\pi/2)\lambda_0}}{i\pi}\int_0^{\infty}e^{-|k_{2\alpha}|r\cosh(\zeta_2)}\cos(\lambda_0\zeta_2)d\zeta_2,\end{aligned} \tag{B3}$$

which except for a factor of i^{-1} is real. Asymptotically,

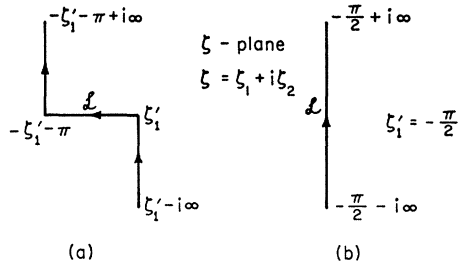

FIG. 7. Contour path for the integral representing the Hankel function.

[25] I am grateful to Dr. F. Mandl for this derivation.

Eq. (B3) becomes

$$H_{i\lambda_0}(i|k_{2\alpha}|r) \xrightarrow[r\to\infty]{} -i\left(\frac{2e^{\pi\lambda_0}}{\pi|k_{2\alpha}|r}\right)^{1/2} e^{-|k_{2\alpha}|r}. \quad \text{(B4)}$$

This demonstrates that $H_{i\lambda_0}{}^{(1)}$ decays exponentially at infinity as required by the wave function $\xi_\alpha(r)$ [Eq. (5.4)].

For small argument at a given $r=r_0$ (i.e., $|k_{2\alpha}|r_0 \ll 1$), an approximate expression for the Hankel function $H_{i\lambda_0}{}^{(1)}(i|k_{2\alpha}|r_0)$ can be easily obtained from the series representation

$$H_{i\lambda_0}{}^{(1)}(i|k_{2\alpha}|r)=\frac{2ie^{(\pi/2)\lambda_0}}{\sinh(\pi\lambda_0)} \times\left\{\sum_{t=0}^{\infty}\frac{(\tfrac{1}{2}|k_{2\alpha}|r)^{2t}\sin[\lambda_0\ln(\tfrac{1}{2}|k_{2\alpha}|r)-\delta_{\lambda_0}(t)]}{t!|\Gamma(t+1+i\lambda_0)|}\right\}, \quad \text{(B5)}$$

where $\delta_{\lambda_0}(t)$ is the argument of the gamma function $\Gamma(t+1+iv)$ defined by the relation

$$\Gamma(t+1+i\lambda_0)=|\Gamma(t+1+i\lambda_0)|\exp[i\delta_{\lambda_0}(t)]. \quad \text{(B6)}$$

Hence

$$H_{i\lambda_0}{}^{(1)}(i|k_{2\alpha}|r_0) \xrightarrow[|k_{2\alpha}|r_0\to 0]{} \frac{2ie^{(\pi/2)\lambda_0}\sin[\lambda_0\ln(\tfrac{1}{2}|k_{2\alpha}|r_0)-\delta_{\lambda_0}(0)]}{|\Gamma(1+i\lambda_0)|\sinh(\pi\lambda_0)}. \quad \text{(B7)}$$

This permits us to write for small argument of the logarithmic derivative of the Hankel function [Eq. (5.8)] at a given radial coordinate $r=r_0$:

$$r_0\left\{\frac{\partial}{\partial r}\ln[r^{1/2}H_{i\lambda_0}{}^{(1)}(i|k_{2\alpha}|r)]\right\}_{r=r_0} \cong\tfrac{1}{2}+\lambda_0\cot[\lambda_0\ln(\tfrac{1}{2}|k_{2\alpha}|r_0)-\delta_{\lambda_0}(0)]. \quad \text{(B8)}$$

It is also desirable to find a small-argument expression for the function

$$\mathcal{Y}(|k_{2\alpha}|r_0)=|r_0{}^{1/2}H_{i\lambda_0}{}^{(1)}(i|k_{2\alpha}|r_0)|^{-2} \times\int_{r_0}^{\infty}|H_{i\lambda_0}{}^{(1)}(i|k_{2\alpha}|r)|^2 rdr \quad \text{(B9)}$$

which appeared in Eq. (6.12). Making use of the relation $[H_{i\lambda_0}{}^{(1)}(i|k_{2\alpha}|r)]^*=-H_{i\lambda_0}{}^{(1)}(i|k_{2\alpha}|r_0)$ and carrying out the integration, we obtain for $\mathcal{Y}(i|k_{2\alpha}|r_0)$ the expression

$$\mathcal{Y}(|k_{2\alpha}|r_0)=\tfrac{1}{2}r_0\{1-|H_{i\lambda_0}{}^{(1)}(i|k_{2\alpha}|r_0)|^{-2}H_{i\lambda_0+1}{}^{(1)} \times(i|k_{2\alpha}|r_0)H_{i\lambda_0-1}{}^{(1)}(i|k_{2\alpha}|r_0)\}. \quad \text{(B10)}$$

For small argument, we have from Eq. (B5)

$$H_{i\lambda_0\pm1}{}^{(1)}(i|k_{2\alpha}|r_0) \xrightarrow[|k_{2\alpha}|r_0\to 0]{} \frac{ie^{(\pi/2)\lambda_0}}{\sinh(\pi\lambda_0)}\left\{\frac{(\tfrac{1}{2}|k_{2\alpha}|r_0)^{1\mp i\lambda_0}}{\Gamma(1\mp i\lambda_0)} +\frac{(\tfrac{1}{2}|k_{2\alpha}|r_0)^{-1\mp i\lambda_0}}{\Gamma(\mp i\lambda_0)}-\frac{(\tfrac{1}{2}|k_{2\alpha}|r_0)^{1\pm i\lambda_0}}{\Gamma(2\pm i\lambda_0)}\right\}. \quad \text{(B11)}$$

Utilizing Eqs. (B7) and (B11), we obtain for $\mathcal{Y}(|k_{2\alpha}|r_0)$ the small-argument expression

$$\mathcal{Y}(|k_{2\alpha}|r_0) \xrightarrow[|k_{2\alpha}|r_0\to 0]{} \left(\frac{|\Gamma(1+i\lambda_0)|^2}{|\Gamma(i\lambda_0)|^2}\right) \times\frac{|k_{2\alpha}|^{-2}}{2r_0\sin^2[\lambda_0\ln(\tfrac{1}{2}|k_{2\alpha}|r_0)-\delta_{\lambda_0}(0)]}. \quad \text{(B12)}$$